

DOCTORAL THESIS

**PHOTOELECTRIC PROCESSES IN  
REACTION CENTER PROTEIN-  
NANOHYBRIDE SYSTEMS**

**Szabó Tibor**

*Supervisors:*

*Dr. László Nagy*

University of Szeged

Faculty of Science and Informatics

Institute of Medical Physics and Informatics

Doctoral School of Physics

Szeged, 2018

## **Introduction**

The photosynthesis is one of the fundamental metabolic processes, that is why it is in the focus of the basic and applied research for decades. We have detailed information about the energy transfer processes after the absorbance of the light, charge separation and –stabilization and about electron and proton transfer mechanisms. Similarly we know the steps of the formation of the chemical potential, the ATP synthesis and the relationship of the structure and the function of the proteins and membranes. That knowledge give us the opportunity to apply it in artificial biosimilar/-mimiking systems. Characteristic molecules of biological systems (proteins, amino acids) are able to solve specific processes with high efficiency, so we have the chance to apply it in it our devices or use it as a model system.

In order to use biological materials in artificial systems we have to make such an environment where they can solve their activity. One opportunity is to make composite materials, where the active component is a biomaterial and the carrier is other organic or inorganic material.

Nowadays the investigation of nanomaterials is also an important scientific question. Intensively investigated and applied nanomaterials are the different carbon derivatives (like carbon nanotubes or grapheme) or nanosized metal or metal-oxide particles. Beneficial properties of nanomaterials (high surface area, special optical properties) qualify them to apply it in composite materials.

With the combination of bio and nanomaterials we can synthesize bionanocomposites, which called as the materials of the future. The advantageous properties make extensively use of bionanocomposites in solar energy conversion, as photodetector, as phototransistor, as herbicide sensor, in fuel cells and in other optoelectronic devices. These materials have a significance in medicine as well, because in reconstitution surgery in some causes we have not got human tissue to replace the damaged or missing parts so we have to use artificial materials. In this situation the biocompatibility is the most important parameter, so the investigation of interaction of bio and inorganic components is extremely important.

## **Aims**

1. Prepare a bionanocomposite material from ITO and RC and determine the spectroscopical and electric properties of it in dried condition.
2. Prepare a conducting polymer layer structure between ITO and silver electrodes and sensitize it with RC. Determine the photoelectric properties and the effect of the RC sensitizer in the system.
3. Use the ITO/MWCNT/RC bionanocomposite in three electrode electrochemical cell as a working electrode and generate light induced photocurrent. Determine the effect of the acceptor and donor type mediator to the system.
4. Prepare an electrochemical cell, where the RC is bound to the working electrode by PTAA conducting polymer. Determine the effect of the polymer to the generated photocurrent.
5. Determine the isotope content of the doped and undoped MWCNT carrier materials. Demonstrate the effect of heteroatoms to the structure of the synthesized MWCNTs.
6. Determine the protein/carrier ratio in MWCNT/RC bionanocomposite with mass spectrometry.
7. Determine the protein/carrier ratio in MWCNT/HRP bionanocomposite with mass spectrometry.

## **Materials and methods**

### **Sample preparation**

Rhodobacter (Rb.) sphaeroides R-26 purple bacterial cells were grown photoheterotrophically. RCs were prepared after solubilization of the photosynthetic membranes by detergent (LDAO, N, N-dimethyldodecylamine-N-oxide, Fluka) and purified by ammonium sulfate precipitation, followed by DEAE Sephacel (Sigma) anion-exchange chromatography. After preparation, the RC

QB site was reconstituted by the addition of ubiquinone-10 (UQ-10, 2,3-dimethoxy-5-methyl-6-decaisoprenol-p-benzoquinone, Sigma) and concentrated by centrifuge filter (Whatman VectaSpin 3, 10 kDa exclusion) to 80–100  $\mu\text{M}$ .

### **Preparation of ITO/RC composite**

For optical spectroscopy, the RC suspension was diluted to 1  $\mu\text{M}$  in detergent suspension (10 mM TRIS, 100 mM NaCl, 0.01% LDAO, pH 8.0). In order to deposit RCs onto ITO the detergent was dialyzed out and calculated amount of purified RCs in the range of  $10^{-6}$  to  $10^{-1}$   $\mu\text{M}$  was dried on the surface of the wafer under the stream of  $\text{N}_2$ .

### **Preparation of nitrogen and sulfur doped CNTs**

During the experiments either Fe(III) – Co(II) / calcium carbonate or nickel(II)-oxide catalysts were used. In this study, a catalyst containing 5 m/m% Fe and 5 m/m% Co was prepared by the impregnation technique. Calculated amounts of Co(II)-acetylacetonate, Fe(III)-acetylacetonate and  $\text{CaCO}_3$  were mixed in a beaker with distilled water. After that a short sonication process was applied to prevent the aggregation of solid precursor particles. Ammonia was added to the system to set the pH to 9, and then the dispersion was placed on a magnetic stirrer and was heated and stirred intensely at  $70^\circ\text{C}$  until most of the solvent had evaporated. After the evaporation, the powder catalyst was dried at  $100^\circ\text{C}$  for 24 h. In case of nickel(II)-oxide catalyst, calculated amount of NiO was dissolved in acetone and the suspension was dropped onto a Si-sheet.

In this study, catalytic chemical vapor deposition (CCVD) method was applied to synthesize nitrogen and sulfur doped multiwalled carbon nanotubes (MWCNTs). Nitrogen and hydrogen gases were passed through the reactor to maintain an inert atmosphere during the synthesis that prevents MWCNTs from oxidation at higher temperatures. The elemental nitrogen gas did not take part in the doping process itself. Therefore, acetylene gas, thiophene and tripropylamine (TPA) were used as carbon, sulfur and nitrogen precursors, respectively. Acetylene and nitrogen

gases were introduced into the system by passing through a Y-shaped junction, while the liquid-phase TPA or thiophene were added by the bubbling technique, where the gases were conducted into liquid TPA or thiophene, before the reactor, thus the gas bubbles carried the TPA or thiophene to the reaction site (Figure 1). For more intense TPA feed, injection method using a syringe pump was also applied; for further experimental details see Szekeres et al. 2015.

In these experiments, 150 mg of catalyst was measured into a quartz boat. After 15 min of leaching, the quartz boat was placed into the oven heated up to 720°C. In the following step, after the reactor was heated, acetylene flow was set to 35 L h<sup>-1</sup> and the MWCNT growing process started. To finalize the synthesis, the acetylene flow rate was set to zero, and after a short-time of leaching, the reactor was cooled down to room temperature to collect the MWCNT samples. In all cases TPA or thiophene was fed into the reactor during the whole reaction time (30 min).

## **Binding RC to MWCNTs**

RC was bound to carboxyl-functionalized MWCNTs by EDC/NHS chemistry procedure. Carboxyl groups of the CNT were activated by the addition of 1-[3-dimethylaminopropyl]-3-ethyl-carbodiimide (EDC). The unstable O-acylisourea ester intermediate compound can be hydrolysed back to the carboxyl form or bound to the amine groups of the RCs, however, the yield of this second reaction route is very low. The addition of N-hydroxysuccinimide (NHS) to the unstable complex an amine-active NHS-ester can be formed opening a very efficient route for the RC binding. After activation, the mixture was dialyzed in potassium phosphate buffer (0.1M, pH 7.0) to remove the unbound activators. Then, the calculated amount of RC solution (typically ca. 100 μM) was added to the activated MWCNT and it was stirred at 4 °C for 3 h. Finally, the sample was separated and washed by an ultracentrifuge until the steady-state absorption spectrum of the supernatant did not show the characteristic peaks of the RC in the near infrared.

## **Binding RC using PTAA polymer**

Binding RCs to PTAA/MWNT complex Amino functionalized MWNTs (0.14 mg ml<sup>-1</sup>) were mixed with PTAA solution (1mgml<sup>-1</sup> in 0.1M phosphate, pH<sup>1/4</sup>8.0) and incubated for 2 h at room temperature. PTAA–MWNT complexes were separated by ultracentrifuge (30000g, 20 min). RC was added to the PTAA/MWNT complex at a final concentration of 65 μM and the detergent was dialyzed out. Finally the RC/PTAA/MWNT complex was separated by ultracentrifuge (30000 g, 20 min).

## **Preparation of MWCNT-RC optoelectronic device**

RC sensitised organic optoelectronic cells were investigated under dry condition. Our sample was prepared by using PEDOT:PSS (poly(3,4-ethylene-dioxythio-phenylene): poly(styrenesulfonate)) and P3HT (poly-(3-hexyl-thiophene)) layers sensitised by the RC proteins. PEDOT:PSS layer was synthesised by electrochemical polymerisation and covered with P3HT-MWCNT-RC complex by spray coating method. P3HT fibre structure was grown on the surface of the MWCNTs [35] and mixed with RCs. Due to the standardized electrochemical deposition the thickness of the PEDOT:PSS layer is quite uniform and approximately 200nm. The thickness of the RC-sensitised layer cannot be given exactly; however, it is expected to be a similar value. Finally, the sample was covered with a silver layer as cathode.

## **An example to apply other protein: Horseradish peroxidase**

The functional groups of carboxyl- functionalized multiwalled carbon nanotubes (f-MCWNTCOOH) (0.14mg/mL) were activated by using crosslinkers N-hydroxysuccinimide (NHS, Sigma-Aldrich) and 1- [3-dimethylaminopropyl]-3-ethyl-carbodiimide (EDC, Sigma-Aldrich). After the activation procedure, the mixture was dialysed in potassium phosphate buffer (PBS, 0.1M, pH 7.0) to remove the excess amount of the crosslinkers. Then the HRP enzyme solution (1 μM, salt free, Reanal) was added to the activated f-MCWNTCOOH suspension and it

was stirred intensively at 4°C for 2h. At the end, the sample was washed until the supernatant did not show enzyme activity and then separated by ultracentrifuge.

## **Methodes**

### **Atomic force microscopy**

In order to visualize the binding of the protein to ITO atomic force microscopy (AFM) investigations were carried out. AFM images were taken with an MFP-3D atomic force microscope (Asylum Research, Santa Barbara, CA). The scanning was performed in AC (tapping) mode with an Olympus cantilever AC160 (Tokyo, Japan) under air dried conditions. The sample was set to the ground potential.

### **Electron microscopy**

Each sample was characterized by transmission electron microscopy (TEM, FEI, Technai G2 20 X-TWIN, 200kV) to study their morphology, which plays a key role in the understanding of the MWCNT doping. The samples were prepared as follows: first a small amount of sample was dispersed in absolute ethanol by ultrasonication (35kHz) in an ultrasonication bath (Transsonic T570/H), then a few drops of the dispersion were placed on a 200 mesh Cu TEM grid with carbon layer.

### **Optical spectroscopy**

Flash-induced absorption changes were measured routinely by a single-beam kinetic spectrophotometer of local design. The P/P+ redox changes of the primary electron donor bacteriochlorophyll dimer (P), and the electrochromic response of the absorption of bacteriopheophytins (BPheo) to the formation of the QA –QB and QAQB – states were detected at 771 nm. Steady state absorption spectra of ITO wafers with or without RCs were measured by Unicam UV4 double beam spectrophotometer in the range of 250–900 nm. In order to minimize the light scattering effect the sample holder close to the detector was used.

## **Measuring conductivity**

Light induced change in the conductivity of RC/ITO composite film was measured by a Keithley 2400s multimeter with seven digits resolution and four points connection. A constant 10 mA current was set and the voltage was measured. Data are represented in ohms. The whole measurement was regulated through the USB port of a computer by using the home developed software. Sample was illuminated by a 250 W tungsten lamp filtered by band-pass filter centered at 400 nm. The infrared component of the excitation light was filtered out.

## **Measurements in electrochemical cells**

Electrochemical cell with three electrodes was designed and fabricated specially for this measurement in our laboratory. ITO covered by the RC sample served as the working electrode and the counter and the reference electrodes were platinum and Ag/AgCl, respectively. UQ-0 and ferrocene, in some experiment as indicated, were used as mediators. Light-induced changes in the cell were measured using a Metrohm PGSTAT204 type potentiostat/galvanostat at ambient temperature. A three-electrode cell construction was used. The working electrode was fabricated from ITO, functionalised CNTs and RCs. The counter and reference electrodes were platinum and Ag/AgCl/3M NaCl, respectively. In some experiments (which is specified in the Results and discussions section) 0.1M NaCl was added or neglected (pH was adjusted to 8.0), or the pH was fixed by the addition of TRIS (20 mM, pH 8.0).

## **Measurements of the radiocarbon contents**

The carbon content of the samples was liberated by sealed tube combustion method. The sample and the MnO<sub>2</sub> oxidant were weighted into a glass tube. When the initial sample was in a liquid matrix it was weighted into the combustion tube and dried with the help of a freeze dryer unit. The quantity of the sample was calculated from the combustion tube with the dried sample and the empty mass of that. The tubes were evacuated to  $<5 \cdot 10^{-3}$  mbar and sealed by a torch. The samples were combusted to CO<sub>2</sub> in a muffle furnace at 550 °C for 48 hours. The gained CO<sub>2</sub> was

purified using a dedicated gas handling system equipped with cryogenic traps in order to remove the other combusted gas components. The quantity of the pure CO<sub>2</sub> was determined in a known volume by high-precision pressure sensor [Janovics 2016]. The yield of the carbon extraction can be calculated from the quantity of the pure CO<sub>2</sub>. The trapped and cleaned CO<sub>2</sub> were converted to graphite by zinc reduction sealed tube graphitization method [Rinyu et al. 2013; Orsovszki and Rinyu 2015]. In the case of less than 100 micrograms carbon, zinc micro-graphitization technique was used [Rinyu et al. 2015].

The measurements of the radiocarbon contents were carried out on a MICADAS type accelerator mass spectrometer [Synal et al. 2004; Synal et al. 2007] in the Institute for Nuclear Research, Debrecen, Hungary [Molnár et al. 2013]. In order to track possible modern carbon contamination during the pretreatment and combustion process, we have extracted chemical standards with well-known radiocarbon activity (IAEA C7 and C8) [Le Clercq et al. 1998] on the same treatment line and measured them together with the samples in the same measurement magazines. BATS AMS data evaluation software was used to treat, process and analyze all of the radiocarbon data [Lukas 2010].

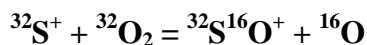
## **Measurement of stable isotope ratios**

Stable isotopes were measured by a Thermo Finnigan DeltaPlusXP isotope ratio mass spectrometer attached to an elemental analyzer (Fisons NA1500 NCS). This EA-IRMS method is based on the rapid oxidation of the sample by flash combustion, which converts all the organic and inorganic substances into combustion products, then the resulted gases are separated in a chromatographic column and detected by the mass spectrometer [Major et al. 2017]. The measured values are expressed in delta notation like  $\delta^{13}\text{C}$  and  $\delta^{15}\text{N}$ , which delta values are defined as follows:  $\delta (\text{‰}) = (\text{R}_{\text{sample}} / \text{R}_{\text{reference}} - 1) * 1000$ , where R is the  $^{13}\text{C}/^{12}\text{C}$ ,  $^{15}\text{N}/^{14}\text{N}$  ratio in the sample or in the international reference material as indicated. The uncertainty of the measurements is 0.2‰ for  $\delta^{13}\text{C}$  and  $\pm 0.3\text{‰}$  for  $\delta^{15}\text{N}$ .

## Measurement of sulfur content

Carbon nanotube samples were digested using a Mars 5 microwave system. 50 mg of the sample were weighted into the Teflon bombs, and they were digested by 2 mL 67% (m/m) nitric acid (suprapure, VWR Chemicals). The applied power was 800 W, 200°C was reached within 20 min, and it was held for 30 min. The samples were transferred into 50 mL volumetric flasks and filled up with ultrapure water.

The analysis of sulfur was performed by Agilent 8800 ICP-QQQ-MS system, using MS/MS mode. Chemical reaction cell (CRC) was operating with oxygen reaction gas. The sulfur was measured with mass-shift, measured on m/z 48.



## New results

1. I bound photosynthetic reaction protein prepared from *Rhodobacter sphaeroides* to indium-tin-oxide surface with drying method. I demonstrated with spectroscopy, the protein keep the activity under dried condition. The resistance of the ITO/RC system decrease under light excitation, because the electron transfer between the two material. The sensitivity of the system is very good, some pM RC cause measurable conductivity change [Szabó és mtsai., **Materials Science and Engineering C, 2012**].
2. It is possible to sensitize organic optoelectronic cell prepared by using PEDOT:PSS (poly(3,4-ethylene-dioxythio-phenylene): poly(styrenesulfonate)) and P3HT (poly-(3-hexyl-thiophene)) layers between ITO and silver electrodes with RC. The cell generates photocurrent under light excitation in dried condition. Selective light excitation proved the sensitizing behavior of the RC [Szabó et al., **Phys. Status Solidi B, 2015**].
3. I bound RC to ITO surface through carbon nanotubes. The composite generate 1 μA photocurrent in electrochemical cell. The measurable photocurrent three times higher if UQ0 acceptor type mediator was added to the system. High ionic strength decrease the rising time of the current

and the affect the accessibility of the RC docking sites [**Szabó et al., Phys. Status Solidi B, 2015**].

4. RC can bind to MWNTs throw PTAA conducting polymer. The MWCNT/PTAA/RC komplex generate photocurrent in electrochemical cell under light excitation. The added mediator affect the magnitude of the photocurrent. The measurable photocurrent is one orders of magnitude higher ( $\mu\text{A}$ ), than apply a non conductive crosslinker, because the PTAA helps the electric connection between the protein and the electrode surface [**Szabó et al., Phys. Status Solidi B, 2012; Szabó et al., Nanoscale Research Letters, 2015**].
5. I investigate the isotope composition of MWCNT/RC komplex with isotope analytical methods. I found out that the  $^{14}\text{C}$  isotopanalitical method give a qualitative information about the protein/carrier ratio. The RC content of the MWCNT/RC complex prepared by EDC-NHS method is 53 wt% [**Szabó és mtsai, Radiocarbon, 2018**].
6. The protein/carrier ratio of the HRP/MWCNT composite is determinable with  $^{14}\text{C}$  isotopanalitical method. The HRP content of the composite is 72 wt% [**Magyar et al., Journal of Nanomaterials, 2016**].

## Publication list

### a, Full papers that the thesis is based on

- 1) **Szabó T**, Magyar M, Nemeth Z, Hernadi K, Endrodi B, Bencsik G, Visy C, Horvath E, Magrez A, Forro L, Nagy L, Charge stabilization by reaction center protein immobilized to carbon nanotubes functionalized by amine groups and poly(3-thiophene acetic acid) conducting polymer, *Phys. Status Solidi B*, 2012, 249(12):2386-2389. IF: 1,49
- 2) **Szabó T**, Bencsik G, Magyar M, Visy C, Gingl Z, Nagy K, Váró G, Hajdu K, Kozák G, Nagy L, Photosynthetic reaction centers/ITO hybrid nanostructure, *Materials Science and Engineering:C*, 2013, 33:769-773. IF: 2,74

- 3) **Szabó T**, Magyar M, Hajdu K, Dorogi M, Nyerki E, Tóth T, Lingvay M, Garab G, Hernádi K, Nagy L, Structural and functional hierarchy in photosynthetic energy conversion - from molecules to nanostructures, *Nanoscale Research Letters*, 2015, 10(1):458. IF: 2,58
- 4) **Szabó T**, Nyerki E, Tóth T, Csekő R, Magyar M, Horváth E, Hernádi K, Endrődi B, Visy C, Forró L, Nagy L, Generating photocurrent by nanocomposites based on photosynthetic reaction centre protein, *Phys. Status Solidi B*, 2015, 252:2614–2619. IF: 1,52
- 5) Magyar M, Rinyu L, Janovics R, Berki P, Hernádi K, Hajdu K, **Szabó T**, Nagy L, Real-Time Sensing of Hydrogen Peroxide by ITO/MWCNT/Horseradish Peroxidase Enzyme Electrode, *Journal of Nanomaterials*, 2016, Article ID 2437873, 11 pages. IF: 1,87
- 6) **Szabó T**, Janovics R, Túri M, Futó I, Papp I, Braun M, Németh K, Szekeres PG, Kinka A, Szabó A, Hernádi K, Hajdu K, Nagy L, Rinyu L, Isotope analytical characterization of carbon based nanocomposites, *Radiocarbon*, 2018, 60(4):1101-1114. IF: 1,81 (2017)

#### **b, Other full papers**

- 1) Hajdu K, **Szabó T**, Magyar M, Bencsik G, Németh Z, Nagy K, Forró L, Váró G, Hernádi K, Nagy L, Photosynthetic reaction center protein in nano structures, *Phys. Status Solidi B*, 2011, 248(11):2700-2703. IF: 1,32
- 2) Magyar M, Hajdu K, **Szabo T**, Hernadi K, Dombi A, Horvath E, Forro L, Nagy L, Long term stabilization of reaction center protein photochemistry by carbon nanotubes, *Phys. Status Solidi B*, 2011, 248(11):2454-2457. IF: 1,32
- 3) Magyar M, Hajdu K, **Szabo T**, Endrodi B, Hernadi K, Horvath E, Magrez A, Forro L, Visy C, Nagy L, Sensing hydrogen peroxide by carbon nanotube/horse radish peroxidase bio-nanocomposite, *Phys. Status Solidi B*, 2013, 250(12):2559-2563. IF: 1,65
- 4) Nagy L, Hajdu K, Torma S, Csikós S, **Szabó T**, Magyar M, Fejes D, Hernádi K, Kellermayer M, Horváth E, Magrez A, Forró L, Photosynthetic reaction centre/carbon nanotube bundle composites, *Phys. Status Solidi B*, 2014, 251(12): 2366-2371. IF: 1,47
- 5) Nagy L, Magyar M, **Szabó T**, Hajdu K, Giotta L, Milano F, Photosynthetic Machineries in Nano-Systems, Special Issue: “Sensors and transducers in the landscape of photosynthesis”, *Current Protein & Peptide Science*, 2014, 15(4): 363-373. IF: 3,15
- 6) Husu I, Magyar M, **Szabó T**, Fiser B, Gómez-Bengoa E, Nagy L, Structure and binding efficiency relations of QB site inhibitors of photosynthetic reaction centres, *Gen. Physiol. Biophys.*, 2015, 34(2):119-33. IF: 0,89

- 7) Nagy L, Kiss V, Brumfeld V, Osvay K, Börzsönyi A, Magyar M, **Szabó T**, Dorogi M, Malkin S, Thermal effects and structural changes of photosynthetic reaction centres characterized by wide frequency band hydrophone: Effect of carotenoids and terbutryne, *Photochemistry and Photobiology*, 2015, 91:1368-1375. IF: 2,01
- 8) Kinka A, Hajdu K, Magyar M, Mucsi L, **Szabó T**, Hernádi K, Horváth E, Magrez A, Forró L, Nagy L, Equilibrium concentration of singlet oxygen in photoreaction of reaction center/carbon nanotube bionanocomposites, *Phys. Status Solidi B*, 2015, 252(11) 2479-2484. IF: 1,52
- 9) Sarrai AE, Hanini S, Kasbadji MN, Tassalit D, **Szabó T**, Hernádi K, Nagy L, Using central composite experimental design to optimize the degradation of Tylosin from aqueous solution by photo-Fenton reaction, *Materials*, 2016, 9(6):428. IF: 2,65
- 10) **Szabó T**, Csekő R, Hajdu K, Nagy K, Sipos O, Galajda P, Nagy L, Sensing photosynthetic herbicides in electrochemical flow cell, *Photosynthesis Research*, 2016, 132(2):127-134. IF: 3,86
- 11) Hajdu K, **Szabó T**, Sarrai AE, Rinyu L, Nagy L, Functional Nanohybrid Materials from Photosynthetic Reaction Center Proteins, *International Journal of Photoenergy*, 2017, Article ID 9128291, 14 pages IF: 1,55

## References

Janovics R. Development of radiocarbon-based measuring methods and their application for nuclear environmental monitoring (PhD thesis, in Hungarian). 2016. University of Debrecen and Hungarian Academy of Sciences Institute for Nuclear Research.

Le Clercq M, Van Der Plicht J, Gröning M, New <sup>14</sup>C reference materials with activities of 15 and 50 pMC, *Radiocarbon*, 1998, 40:295-297.

Liu J, Zou J, Zhai L, Bottom-up Assembly of Poly(3-hexylthiophene) on Carbon Nanotubes: 2D Building Blocks for Nanoscale Circuits, *Macromol Rapid Commun.*, 2009, 30:1387-1391.

Molnár M, Rinyu L, Veres M, Seiler M, Wacker L, Synal HA, EnvironMICADAS: A mini <sup>14</sup>C AMS with enhanced gas ion source interface in the Hertelendi Laboratory on Environmental Studies (HEKAL). *Radiocarbon*, 2013, 55(2):338-44.

Major I, Gyökös B, Túri M, Futó I, Filep Á, Hoffer A, Furu E, Jull AJT, Molnár M, Evaluation of an automated EA-IRMS method for total carbon analysis of atmospheric aerosol at HEKAL. *Journal of Atmospheric Chemistry*, 2017, 75(1):85-96.

Orsovszki G, Rinyu L, Flame-sealed tube graphitization using zinc as the sole reduction agent: Precision improvement of EnvironMICADAS <sup>14</sup>C measurements on graphite targets, *Radiocarbon*, 2015, 57:979-990.

Rinyu L, Molnár M, Major I, Nagy T, Veres M, Kimák Á, Wacker L, Synal HA, Optimization of sealed tube graphitization method for environmental C-14 studies using MICADAS, *Nuclear Instruments and Methods in Physics Research B*, 2013, 294:270-275.

Rinyu L, Orsovszki G, Futó I, Veres M, Molnár M, Application of zinc sealed tube graphitization on sub-milligram samples using EnvironMICADAS. *Nuclear Instruments and Methods in Physics Research Section B.*, 2015, 361:406-413.

Synal HA, Döbeli M, Jacob S, Stocker M, Suter M, Radiocarbon AMS towards its lower-energy limits, *Nuclear Instruments and Methods in Physics Research B.*, 2004, 223-224:339-345.

Synal HA, Stocker M, Suter M, MICADAS: A new compact radiocarbon AMS system, *Nuclear Instruments and Methods in Physics Research B.*, 2007, 259:7-13.

Szekeres GP, Nemeth K, Kinka A, Magyar M, Reti B, Controlled nitrogen doping and carboxyl functionalization of multi-walled carbon nanotubes. *Phys. Status Solidi B.*, 2015, 252:2472-2478.

Wacker L, Christl M, Synal HA, Bats: A new tool for AMS data reduction, *Nuclear Instruments and Methods in Physics Research Section B: Beam Interactions with Materials and Atoms*, 2010, 268:976-979.